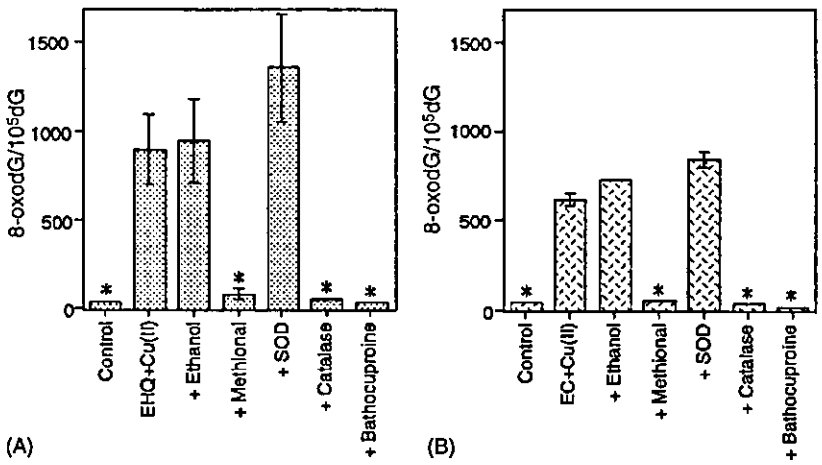

Fig. 5. Effects of reactive oxygen species scavengers and bathocuproine on 8-oxodG formation induced by EHQ or EC. Reaction mixture contained calf thymus DNA (50 μM/base), 20 μM $CuCl_2$, 25 μM EHQ (A) or EC (B) and scavenger in 4 mM sodium phosphate buffer (pH 7.8) containing 5 μM DTPA. Scavenger was added to the positive control (EHQ + Cu(II) (A) and EC + Cu(II) (B)) where indicated. The concentration of scavengers and metal chelator was as follows: 5% (v/v) ethanol; 0.1 M methional; 50 units of SOD; 50 units of catalase; 50 μM bathocuproine. Control does not contain EHQ or EC. Results were obtained from three independent experiments. $^{*}P < 0.05$, significant decrease compared with the positive control, evaluated by *t*-test or Welch test. Values are expressed as means ± S.D.

mation. However, SOD slightly facilitated 8-oxodG formation.

3.6. Involvement of O_2^- in 8-oxodG formation

Generation of O_2^- in the 8-oxodG formation was investigated by measuring the extent of cytochrome *c* reduction. As shown in Fig. 6, O_2^- was generated in the reaction system containing EHQ or EC under the aerobic condition, suggesting the involvement of O_2^- in the mechanism of oxidative DNA damage. EHQ induced about two-fold larger generation of O_2^- compared with EC.

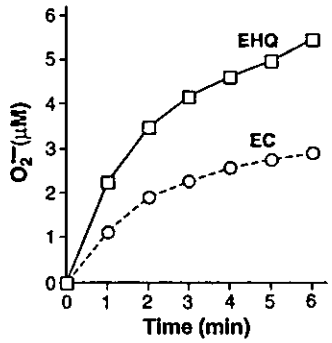

Fig. 6. O_2^--generation from EHQ or EC. The reaction mixture containing 40 μM ferricytochrome *c*, 100 μM EHQ or EC, 2.5 μM DTPA in 1 ml of 10 mM sodium phosphate buffer (pH 7.8) with or without SOD (100 units) was incubated at 37 °C. The amount of O_2^- was determined by the measurement of cytochrome *c* reduction as described in Section 2.

3.7. Stoichiometry of the reaction between ethylbenzene metabolites and Cu(II)

We investigated molar ratio of these ring-dihydroxylated metabolites (EHQ or EC) and Cu(II) in the redox reaction by measuring the absorbance of Cu(I)-bathocuproine complex (Fig. 7). Twenty-five micromolars of EHQ or EC were necessary for the complete reduction of 50 μM of Cu(II). This result implies a 2:1 stoichiometry for the reduction of Cu(II) by ethylbenzene metabolites.

4. Discussion

The present study has firstly demonstrated that EHQ and EC are formed by microsomes from rat liver as novel metabolites of ethylbenzene via generation of 2-ethylphenol and 4-ethylphenol, respectively. EC has been detected as a metabolite of ethylbenzene in bacteria [20]. Recent studies have suggested that CYP2E1 is

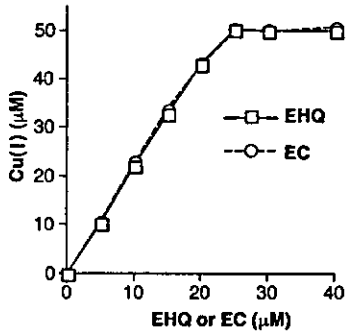

Fig. 7. Stoichiometry of the reaction between ethylbenzene metabolites and Cu(II). Calculated amounts of reduced Cu against EHQ and EC are shown based on the absorbance of the Cu(I)–bathocuproine complex as described in Section 2. The reaction mixture contains 50 μM $CuCl_2$.

the major enzyme to metabolize ethylbenzene [21,22]. Sams et al. have demonstrated that CYP2E1 catalyzes the side-chain hydroxylation of ethylbenzene to produce 1-phenylethanol [21]. 2-Ethylphenol and 4-ethylphenol are minor metabolites of ethylbenzene formed through ring hydroxylation [6,11,23]. Previous studies have demonstrated that benzene undergoes CYP2E1-catalyzed ring hydroxylation to generate toxic metabolites, such as hydroquinone, catechol and benzoquinone [24,25]. Therefore, the generation of two ring-dihydroxylated metabolites, EHQ and EC, may be primarily catalyzed by CYP2E1. This idea is supported by a recent study showing that CYP2E1 is involved in ethylbenzene metabolism to form the compounds capable of generating reactive oxygen species [22]. In this study, EHQ and EC caused oxidative DNA damage including 8-oxodG in the presence of Cu(II). EHQ formed approximately two-fold larger amount of 8-oxodG compared with EC. This result can be explained by the observation that EHQ generated about two-fold larger amount of O_2^- compared with EC. Furthermore, NADH enhanced Cu(II)-mediated DNA damage and the 8-oxodG formation induced by EC. 8-OxodG is not only as a significant biomarker for oxidative DNA damage, but also as an inducer for another intramolecular base damage in the DNA strand under oxidative stress [26]. Numerous studies have indicated that the formation of 8-oxodG causes misreplication of DNA, leading to mutation and cancer [27,28]. The kidney and testis are target organs for carcinoma induction by ethylbenzene. This can be explained by assuming that ethylbenzene metabolites produced in the liver are transported to target organs. CYPs are also expressed in the kidney [29], where toxic metabolites can be produced. The testis is highly susceptible to oxidative damage, since this organ has low activity of catalase [30]. Thus, it would be possible that the oxidative DNA damage mediated by CYP-catalyzed metabolites of ethylbenzene is involved in carcinogenesis in these organs.

Copper is present in nucleus and closely associated with chromosomes and bases [31,32]. Although mammals have evolved means of minimizing levels of free copper ions and most copper ions bind to protein carriers and transporters [33], free copper ions may participate in ROS generation under certain conditions. The level (20 μM) of free copper ions used in this study may be higher than the physiological concentrations. In our experimental conditions, DNA was treated with ethylbenzene metabolites and Cu(II) for a short time. The conditions would be relevant to the lifetime exposure of human to low level of free copper ions. NADH concentration in tissues was estimated to be as high as that applied in our in vitro system [34]. Therefore, Cu(II) and NADH may play significant roles in the mechanism of ethylbenzene metabolites-mediated DNA damage in vivo. Complete inhibition of 8-oxodG formation by Cu(I)-specific chelator suggests Cu(II) reduction coupled to the autoxidation of EHQ and EC. The significant inhibition by catalase indicates the participation of H_2O_2 in DNA damage. Generation of O_2^- in the reaction system containing the ring-dihydroxylated metabolites is consistent with the result that SOD enhances 8-oxodG formation, assuming that DNA damage is caused by H_2O_2 derived from O_2^- generated concomitantly in the reaction of these metabolites and Cu(II). Inhibitory effect of methional supports the formation of a reactive species other than hydroxyl radical, such as copper–hydroperoxo complex (Cu(I)OOH). Based on these results, we propose a possible mechanism of the Cu(II)-mediated DNA damage by ethylbenzene metabolites as shown in Fig. 8. EHQ undergoes Cu(II)-mediated autoxidation to the corresponding semiquinone radical and subsequently to ethylbenzoquinone. Similarly, EC undergoes Cu(II)-mediated autoxidation to semiquinone radical and then 4-ethyl-1,2-benzoquinone. The hypothesis that these ethylbenzene metabolites undergo two steps of Cu(II)-mediated autoxidation is confirmed by a 2:1 stoichiometry for

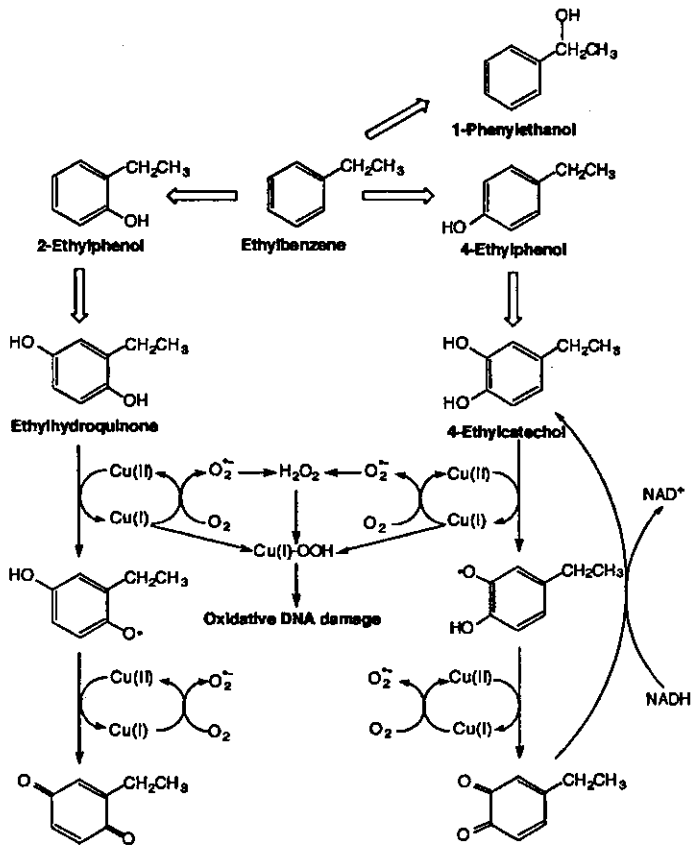

Fig. 8. Possible mechanism of oxidative DNA damage induced by EHQ and EC.

the reduction of Cu(II) by ethylbenzene metabolites. This result simply reflects the mechanism by which the maximum number of electrons are transferred to Cu(II) during autoxidation of EHQ and EC. On the other hand, abilities to cause DNA damage may depend on redox potentials of EHQ and EC. During the autoxidation, Cu(II) is reduced to Cu(I) and O_2^- is generated from O_2 by the reaction with the Cu(I). O_2^- is dismutated into H_2O_2 and interact with Cu(I) to form DNA–Cu(I)OOH complex [35]. There remains a possibility that DNA damage is induced by hydroxyl radical generated in very proximity to the DNA, i.e. in the DNA–Cu(I)OOH complex, before being scavenged [36].

We showed that EC-induced Cu(II)-mediated DNA damage more efficiently than EHQ in the presence of NADH. This result suggests that 4-ethyl-1,2-benzoquinone is again reduced to EC by NADH, and forms a redox cycle in which large amount of O_2^- is produced. Similar effects of NADH were observed with benzene metabolites, catechol. Hirakawa et al. [37] indicated that 1,2-benzoquinone was converted directly into catechol through a nonenzymatic two-electron reduction by NADH. The reduction of 1,2-benzoquinone by NADH proceeds more rapidly than that of 1,4-benzoquinone. Similarly, 4-ethyl-1,2-benzoquinone appears to be converted to 1,2-benzoquinone through NADH-mediated two-electron reduction. This reduction of 4-ethyl-1,2-benzoquinone accelerates the redox reaction, resulting in the enhancement of DNA damage. We previously demonstrated that methylcatechols, toluene metabolites, caused Cu(II)-mediated DNA damage, which was more efficiently enhanced by NADH compared with methylhydroquinone, an another toluene metabolite [38,39]. The generation of reactive oxygen

species from redox reaction contributes to carcinogenesis caused by a variety of air pollutants, such as ethylbenzene, benzene and toluene.

This is the first report that DNA damaging active compounds, EHQ and EC were detected in ethylbenzene metabolism. These metabolites have not been noticed as the causes of ethylbenzene-mediated carcinogenesis probably because of their limited production. Nevertheless, oxidative stress provided in the redox cycle containing these metabolites would be a key in the carcinogenesis mechanism of ethylbenzene.

Acknowledgement

This work was partly supported by Grants-in-Aid for Scientific Research from the Ministry of Education, Science, Sports and Culture of Japan.

References

[1] Z. Bardodej, E. Bardodejova, Biotransformation of ethyl benzene, styrene, and α-methylstyrene in man, Am. Ind. Hyg. Assoc. J. 31 (1970) 206–209.
[2] J.P. Gromiec, J.K. Piotrowski, Urinary mandelic acid as an exposure test for ethylbenzene, Int. Arch. Occup. Environ. Health 55 (1984) 61–72.
[3] B.H. Chin, J.A. McKelvey, T.R. Tyler, L.J. Calisti, S.J. Kozbelt, L.J. Sullivan, Absorption, distribution, and excretion of ethylbenzene, ethylcyclohexane, and methylethylbenzene isomers in rats, Bull. Environ. Contam. Toxicol. 24 (1980) 477–483.
[4] I.J. Climie, D.H. Hutson, G. Stoydin, The metabolism of ethylbenzene hydroperoxide in the rat, Xenobiotica 13 (1983) 611–618.
[5] P.C. Chan, J.K. Hasemani, J. Mahleri, C. Aranyi, Tumor induction in F344/N rats and B6C3F1 mice following inhalation exposure to ethylbenzene, Toxicol. Lett. 99 (1998) 23–32.
[6] IARC Working Group, Ethylbenzene, in: IARC Monographs on the Evaluation of Carcinogenic Risks to Humans, vol. 77, IARC Press, Lyon, 2000, 227–266.
[7] S. Kawanishi, Y. Hiraku, S. Oikawa, Mechanism of guanine-specific DNA damage by oxidative stress and its role in carcinogenesis and aging, Mutat. Res. 488 (2001) 65–76.
[8] S. Kawanishi, Y. Hiraku, M. Murata, S. Oikawa, The role of metals in site-specific DNA damage with reference to carcinogenesis, Free Radic. Biol. Med. 32 (2002) 822–832.
[9] S. Kawanishi, S. Oikawa, Y. Hiraku, S. Inoue, Oxidative DNA damage by interaction of carcinogen with metal, in: V.-P. Kotsaki-Kovatsi, A.J. Vafiadou (Eds.), Aspects on Environmental Toxicology, Thessaloniki University Press, 1995, pp. 377–381.
[10] National Toxicology Program, Toxicology and carcinogenesis studies of α-methylbenzyl alcohol (CAS No. 98-85-1) in F344/N rats and B6C3F1 mice (Gavage Studies), in: Tech. Rep. Ser. No. 369; NIH Publ. No. 89-2824, Research Triangle Park, NC, 1990.
[11] K.M. Engström, Metabolism of inhaled ethylbenzene in rats, Scand. J. Work. Environ. Health 10 (1984) 83–87.
[12] M.F. Denissenko, A. Pao, M. Tang, G.P. Pfeifer, Preferential formation of benzo[*a*]pyrene adducts at lung cancer mutational hotspots in P53, Science 274 (1996) 430–432.
[13] D. Sidransky, A. Von Eschenbach, Y.C. Tsai, P. Jones, I. Summerhayes, F. Marshall, M. Paul, P. Green, S.R. Hamilton, P. Frost, B. Vogelstein, Identification of p53 gene mutations in bladder cancers and urine samples, Science 252 (1991) 706–709.
[14] H. Yoshimura, N. Ozawa, S. Saeki, Inductive effect of polychlorinated biphenyls mixture and individual isomers on the hepatic microsomal enzymes, Chem. Pharm. Bull. (Tokyo) 26 (1978) 1215–1221.
[15] T. Omura, R. Sato, The carbon monoxide-binding pigment of liver microsomes. I. Evidence for its hemoprotein nature, J. Biol. Chem. 239 (1964) 2370–2378.
[16] P. Chumakov, EMBL Data Library, Accession Number X54156, 1990.
[17] M. Murata, S. Kawanishi, Oxidative DNA damage by vitamin A and its derivative via superoxide generation, J. Biol. Chem. 275 (2000) 2003–2008.
[18] K. Ito, S. Inoue, K. Yamamoto, S. Kawanishi, 8-Hydroxydeoxyguanosine formation at the 5′ site of 5′-GG-3′ sequences in double-stranded DNA by UV radiation with riboflavin, J. Biol. Chem. 268 (1993) 13221–13227.
[19] D. Blair, H. Diehl, Bathophenanthrolinedisulphonic acid and bathocuproinedisulphonic acid, water soluble reagents for iron and copper, Talanta 7 (1961) 163–174.
[20] D.T. Gibson, B. Gschwendt, W.K. Yeh, V.M. Kobal, Initial reactions in the oxidation of ethylbenzene by *Pseudomonas putida*, Biochemistry 12 (1973) 1520–1528.
[21] C. Sams, G.D. Loizou, J. Cocker, M.S. Lennard, Metabolism of ethylbenzene by human liver microsomes and recombinant human cytochrome P450s (CYP), Toxicol. Lett. 147 (2004) 253–260.
[22] S.C. Serron, N. Dwivedi, W.L. Backes, Ethylbenzene induces microsomal oxygen free radical generation: antibody-directed characterization of the responsible cytochrome P450 enzymes, Toxicol. Appl. Pharmacol. 164 (2000) 305–311.
[23] K.M. Engström, Urinalysis of minor metabolites of ethylbenzene and *m*-xylene, Scand. J. Work. Environ. Health 10 (1984) 75–81.
[24] I. Gut, V. Nedelcheva, P. Soucek, P. Stopka, P. Vodicka, H.V. Gelboin, M. Ingelman-Sundberg, The role of CYP2E1 and 2B1 in metabolic activation of benzene derivatives, Arch. Toxicol. 71 (1996) 45–56.
[25] M.J. Seaton, P.M. Schlosser, J.A. Bond, M.A. Medinsky, Benzene metabolism by human liver microsomes in relation to cytochrome P450 2E1 activity, Carcinogenesis 15 (1994) 1799–1806.
[26] J.E. Kim, S. Choi, J.A. Yoo, M.H. Chung, 8-Oxoguanine induces intramolecular DNA damage but free 8-oxoguanine pro-

tects intermolecular DNA from oxidative stress, FEBS Lett. 556 (2004) 104–110.
[27] S. Shibutani, M. Takeshita, A.P. Grollman, Insertion of specific bases during DNA synthesis past the oxidation-damaged base 8-oxodG, Nature 349 (1991) 431–434.
[28] K.C. Cheng, D.S. Cahill, H. Kasai, S. Nishimura, L.A. Loeb, 8-Hydroxyguanine, an abundant form of oxidative DNA damage, causes G–T and A–C substitutions, J. Biol. Chem. 267 (1992) 166–172.
[29] X. Zhao, J.D. Imig, Kidney CYP450 enzymes: biological actions beyond drug metabolism, Curr. Drug Metab. 4 (2003) 73–84.
[30] A. Zini, P.N. Schlegel, Catalase mRNA expression in the male rat reproductive tract, J. Androl. 17 (1996) 473–480.
[31] B.H. Geierstanger, T.F. Kagawa, S.L. Chen, G.J. Quigley, P.S. Ho, Base-specific binding of copper(II) to Z-DNA. The 1.3-Å single crystal structure of d(m5CGUAm5CG) in the presence of $CuCl_2$, J. Biol. Chem. 266 (1991) 20185–20191.
[32] S.E. Bryan, D.L. Vizard, D.A. Beary, R.A. LaBiche, K.J. Hardy, Partitioning of zinc and copper within subnuclear nucleoprotein particles, Nucl. Acids Res. 9 (1981) 5811–5823.
[33] M.C. Linder, Copper and genomic stability in mammals, Mutat. Res. 475 (2001) 141–152.
[34] A. Uppal, P.K. Gupta, Measurement of NADH concentration in normal and malignant human tissues from breast and oral cavity, Biotechnol. Appl. Biochem. 37 (2003) 45–50.
[35] K. Ito, K. Yamamoto, S. Kawanishi, Manganese-mediated oxidative damage of cellular and isolated DNA by isoniazid and related hydrazines: non-Fenton-type hydroxyl radical formation, Biochemistry 31 (1992) 11606–11613.
[36] M. Dizdaroglu, G. Rao, B. Halliwell, E. Gajewski, Damage to the DNA bases in mammalian chromatin by hydrogen peroxide in the presence of ferric and cupric ions, Arch. Biochem. Biophys. 285 (1991) 317–324.
[37] K. Hirakawa, S. Oikawa, Y. Hiraku, I. Hirosawa, S. Kawanishi, Catechol and hydroquinone have different redox properties responsible for their differential DNA-damaging ability, Chem. Res. Toxicol. 15 (2002) 76–82.
[38] N. Nakai, M. Murata, M. Nagahama, T. Hirase, M. Tanaka, T. Fujikawa, N. Nakao, K. Nakashima, S. Kawanishi, Oxidative DNA damage induced by toluene is involved in its male reproductive toxicity, Free Radic. Res. 37 (2003) 69–76.
[39] M. Murata, M. Tsujikawa, S. Kawanishi, Oxidative DNA damage by minor metabolites of toluene may lead to carcinogenesis and reproductive dysfunction, Biochem. Biophys. Res. Commun. 261 (1999) 478–483.

Available online at www.sciencedirect.com
SCIENCE DIRECT
Cancer Letters 215 (2004) 141–150
CANCER Letters
www.elsevier.com/locate/canlet

Mechanism of carcinogenesis induced by a veterinary antimicrobial drug, nitrofurazone, via oxidative DNA damage and cell proliferation

Yusuke Hiraku[a], Aki Sekine[a], Hiromi Nabeshi[a], Kaoru Midorikawa[a], Mariko Murata[a], Yoshito Kumagai[b], Shosuke Kawanishi[a,*]

[a]*Department of Environmental and Molecular Medicine, Mie University School of Medicine, 2-174 Edobashi, Tsu, Mie 514-8507, Japan*
[b]*Department of Environmental Medicine, Institute of Community Medicine, University of Tsukuba, 1-1-1 Tennodai, Tsukuba, Ibaraki 305-8575, Japan*

Received 30 December 2003; received in revised form 17 May 2004; accepted 18 May 2004

Abstract

Nitrofurazone, a veterinary antimicrobial drug, causes mammary and ovarian tumors in animals. We investigated the mechanisms of carcinogenesis by nitrofurazone. Nitrofurazone significantly stimulated the proliferation of estrogen-dependent MCF-7 cells. Nitrofurazone caused Cu(II)-mediated damage to ^{32}P-5′-end-labeled DNA fragments obtained from human genes only when cytochrome P450 reductase was added. DNA damage was inhibited by catalase and bathocuproine. DNA damage was preferably induced at the 5′-A*CG*-3′ sequence, a hotspot of the *p*53 gene. These findings suggest that nitrofurazone metabolites are involved in tumor initiation through oxidative DNA damage and nitrofurazone itself enhances cell proliferation, leading to promotion and/or progression in carcinogenesis.

Keywords: Nitrofurazone; Estrogenic activity; DNA damage; Cytochrome P450 reductase; Initiation; Promotion

1. Introduction

The use of antimicrobial drugs in animal husbandry and residues of these drugs in animal food may pose a risk to human health. Various nitro compounds, including nitrofurazone, furazolidone, nitrofurantoin and metronidazole, have been used as veterinary antimicrobial drugs. These compounds have been reported to cause tumors in experimental

Abbreviations: 8-oxodG, 8-oxo-7,8-dehydro-2′-deoxyguanosine; HPLC-ECD, high performance liquid chromatograph equipped with an electrochemical detector; DTPA, diethylenetriamine-*N*,*N*,*N*′,*N*″,*N*″-pentaacetic acid; SOD, superoxide dismutase; E_2, 17β-estradiol; Fpg, formamidopyrimidine-DNA glycosylase; $^{\cdot}OH$, hydroxyl free radical; H_2O_2, hydrogen peroxide; $O_2^{\cdot-}$, superoxide anion radical.

* Corresponding author. Tel./fax: +81-59-231-5011.
E-mail address: kawanisi@doc.medic.mie-u.ac.jp (S. Kawanishi).

0304-3835/$ - see front matter © 2004 Elsevier Ireland Ltd. All rights reserved.
doi:10.1016/j.canlet.2004.05.016

animals and suspected to be carcinogenic to humans [1–4]. Nitrofurazone is a broad-spectrum antimicrobial drug used both therapeutically and prophylactically in a number of food-producing species. Nitrofurazone has been detected in muscle, liver and milk of animals [5,6]. National Toxicology Program has provided clear evidence of carcinogenic activity of nitrofurazone for female rats and mice [7]. Nitrofurazone increased the incidences of mammary tumors in female rats and ovarian tumors in female mice [8]. Nitrofurazone induced promotion of mammary tumor growth in rats treated with a carcinogen [9]. It has been proposed that alteration in endocrine function may participate in nitrofurazone-induced carcinogenesis [9,10]. The increase in serum prolactin and progesterone concentrations was observed in nitrofurazone-treated rats [9]. However, the mechanisms of carcinogenesis induced by nitrofurazone have not been well understood.

A variety of nitro compounds are enzymatically reduced in biological systems [11,12]. There is a significant correlation between nitrofurazone reduction and the amount of cellular DNA damage [13]. Therefore, nitrofurazone metabolites generated via reductive activation may participate in carcinogenesis by causing DNA damage. Alternatively, estrogenic activity of nitrofurazone may also contribute to carcinogenesis. It is well known that estrogen causes cancers in female reproductive organs such as breast and uterus [14]. Thus, nitrofurazone, which causes mammary and ovarian tumors, may have estrogenic activity.

We have recently reported that estrogen metabolites induce oxidative DNA damage, whereas estrogen itself enhances cell proliferation [15]. This result leads to an idea that in the case of nitrofurazone, these two distinct mechanisms may cooperatively contribute to carcinogenesis: DNA damage induced by its metabolites and enhancement of cell proliferation by nitrofurazone itself. DNA damage was examined using ^{32}P-5′-end-labeled DNA fragments obtained from human cancer-relevant genes in the presence of NADPH-dependent cytochrome P450 reductase. We measured the content of 8-oxo-7,8-dehydro-2′-deoxyguanosine (8-oxodG), an indicator of oxidative DNA damage using a high performance liquid chromatograph equipped with an electrochemical detector (HPLC-ECD). To elucidate the mechanism of DNA damage, we utilized electron spin resonance (ESR) spectroscopy to investigate the generation of radicals from nitrofurazone. To evaluate the estrogenic activity, we examined the effect of nitrofurazone on proliferation of estrogen-dependent MCF-7 cells derived from human breast cancer (E-Screen test).

2. Materials and methods

2.1. Materials

A restriction enzyme (*Hin*dIII) and T_4 polynucleotide kinase were purchased from New England Biolabs (Beverly, MA, USA). [γ-^{32}P]-ATP (222 TBq/mmol) was from New England Nuclear (Boston, MA, USA). Restriction enzymes (*Eco*RI and *Apa*I) and calf intestine phosphatase were from Roche (Mannheim, Germany). Nitrofurazone was purchased from Aldrich Chemical Co. (Milwaukee, WI, USA). Superoxide dismutase (SOD, 3000 units/mg from bovine erythrocytes), catalase (45,000 units/mg from bovine liver), 17β-estradiol (E_2) and bacterial alkaline phosphatase (BAP) were purchased from Sigma Chemical Co. (St. Louis, MO, USA). Nuclease P_1 was from Yamasa Shoyu Co. (Chiba, Japan). *E. coli* formamidopyrimidine-DNA glycosylase (Fpg) was obtained from Trevigen Inc. (Gaithersburg, MD, USA).

2.2. Bioassay for measuring estrogenicity of nitrofurazone (E-Screen test)

The E-Screen test was performed by the method reported previously [15–17]. Human estrogen-sensitive breast cancer MCF-7 (estrogen receptor-positive) and nontumorigenic mammary epithelial MCF-10A cells (estrogen receptor-negative) (American Type Culture Collection, Manassas, VA, USA) were plated into 12-well plates at an initial concentration of 30,000 cells/well. Cells were allowed to attach for 24 h and then the seeding medium was replaced with the experimental medium as described previously [17]. The cells were incubated with nitrofurazone for 6 days, and then harvested cells were counted using a Coulter Counter.

2.3. Preparation of cytochrome P450 reductase

Cytochrome P450 reductase was purified from Triton N-101-solubilized liver microsomes from Phenobarbital-treated rats as described previously [18]. The purified enzyme showed a single band (76 kDa) on SDS-PAGE with a specific activity to reduce 35 μmol/mg/min of cytochrome *c*.

2.4. Preparation of ^{32}P-5′-end-labeled DNA fragments

DNA fragments were obtained from the human *p53* tumor suppressor gene [19]. The ^{32}P-end-labeled 650-base pair DNA fragment (*Hin*dIII* 13972-*Eco*RI* 14621, asterisk indicates ^{32}P-labeling) was obtained as described previously [20]. The 650-base pair fragment was digested with *Apa*I to obtain a singly labeled 443-base pair (*Apa*I 14179-*Eco*RI* 14621) and a 211-base pair (*Hin*dIII* 13972-*Apa*I 14182) fragments.

2.5. Detection of damage to ^{32}P-labeled DNA fragments

The reaction mixture in a microtube (1.5-ml Eppendorf), containing nitrofurazone, 100 μM NADPH and 2.1 μg/ml cytochrome P450 reductase in 20 mM potassium phosphate buffer (pH 7.4), was preincubated for 30 min at 25 °C. Then, ^{32}P-DNA fragment, 10 μM/base sonicated calf thymus DNA and 20 μM $CuCl_2$ (final concentration) were added, and the mixture was incubated at 37 °C. Subsequently, DNA was treated with 1 M piperidine for 20 min at 90 °C or 6 units of Fpg protein in the reaction buffer (10 mM HEPES–KOH (pH 7.4), 100 mM KCl, 10 mM EDTA and 0.1 mg/ml BSA) for 2 h at 37 °C. Fpg protein catalyzes the excision of 8-oxodG as well as Fapy residues [21]. The preferred cleavage sites were determined by direct comparison of the positions of the oligonucleotides with those produced by the chemical reactions of the Maxam–Gilbert procedure [22] using a DNA-sequencing system (LKB 2010 Macrophor). A laser densitometer (Personal Densitometer SI, Amarsham Biosciences) was used for the measurement of the relative amounts of oligonucleotides from the treated DNA fragments.

2.6. Measurement of 8-oxodG formation in calf thymus DNA by nitrofurazone

The amount of 8-oxodG was measured by a modified method of Kasai et al. [23]. The reaction mixture containing nitrofurazone, 100 μM NADPH and 2.1 μg/ml cytochrome P450 reductase in 4 mM potassium phosphate buffer (pH 7.4), was preincubated for 30 min at 25 °C. Then, 100 μM/base calf thymus DNA and 20 μM $CuCl_2$ were added, and the mixture was incubated for 30 min at 37 °C. After incubation, diethylenetriamine-*N,N,N′,N″,N″*-pentaacetic acid (DTPA) was added to stop the reaction at the final concentration of 0.1 mM. After ethanol precipitation, DNA was digested to the nucleosides with nuclease P_1 and calf intestine phosphatase, and analyzed with an HPLC-ECD as described previously [24].

2.7. Analysis of 8-oxodG formation in cultured cells treated with nitrofurazone

HL-60 cells (1.0×10^6 cells/ml) were incubated with nitrofurazone in RPMI 1640 supplemented with 6% fetal calf serum for 4 h at 37 °C. Then, the cells were treated with RNase and proteinase K in lysis buffer (Applied Biosystems) under the anaerobic condition as described previously [25]. After ethanol precipitation, DNA was digested with nuclease P_1 and BAP, and then analyzed by an HPLC-ECD.

2.8. Statistical analysis

For statistical analysis of the data, Student's *t*-test was used at a significance level of $P<0.05$. The data represent means ± SD.

2.9. Electron spin resonance studies

ESR spectra were measured at room temperature (25 °C), using a JES-TE-100 (JEOL, Tokyo, Japan) spectrometer with 100-kHz field modulation. Spectra were recorded at room temperature with microwave power of 10 mW, modulation amplitude of 0.1 mT, receiver gain of 1000, time constant of 0.1 s and sweep time of 4 min. Magnetic fields were calculated using the splitting of Mn(II) in MgO (ΔH_{3-4}= 8.69 mT).

3. Results

3.1. Estrogenic activity of nitrofurazone

Fig. 1 shows an effect of nitrofurazone on proliferation of MCF-7 and MCF-10A cells. Nitrofurazone increased the number of MCF-7 cells in a dose-dependent manner (Fig. 1A). Nitrofurazone significantly enhanced proliferation of MCF-7 cells at 100 nM ($P<0.05$) and 1–10 μM ($P<0.001$), although the estrogenic activity of nitrofurazone was slightly smaller than that of 100 pM E_2 (Fig. 1A). Nitrofurazone as well as E_2 did not increase the number of MCF-10A cells compared with nontreated control (Fig. 1B).

3.2. Damage to ^{32}P-labeled DNA fragments by nitrofurazone plus cytochrome P450 reductase

Fig. 2 shows the autoradiogram of DNA damage induced by nitrofurazone and effects of scavengers and bathocuproine. In the presence of both cytochrome P450 reductase and Cu(II), nitrofurazone-induced DNA damage in dose- (Fig. 2A) and time-dependent manners (data not shown), whereas nitrofurazone did not cause damage when the enzyme (Fig. 2A) or Cu(II) (data not shown) was omitted. Piperidine treatment enhanced DNA damage, suggesting that not only strand breakage but also base modification and/or liberation were induced (data not shown). Fpg treatment also enhanced nitrofurazone-induced DNA damage, suggesting that base modification, particularly 8-oxodG formation, a highly mutagenic lesion [21], was induced (data not shown). DNA damage was inhibited by catalase and bathocuproine, suggesting that hydrogen peroxide (H_2O_2) and Cu(I) were involved. Typical hydroxyl free radical ($^{\cdot}OH$) scavengers, ethanol, mannitol, sodium formate and methional, did not inhibit DNA damage. SOD showed little or no inhibitory effect on DNA damage.

3.3. Site specificity of DNA damage induced by nitrofurazone

Fig. 3 shows the site specificity of DNA damage induced by nitrofurazone. Nitrofurazone induced damage to the DNA fragments obtained from the human *p53* gene particularly at thymine and cytosine. Nitrofurazone induced a double base lesion consisting of piperidine-labile cytosine lesion and Fpg-sensitive guanine lesion at the 5′-A*CG*-3′ sequence, complementary to codon 273 in the *p53* gene, a known hotspot.

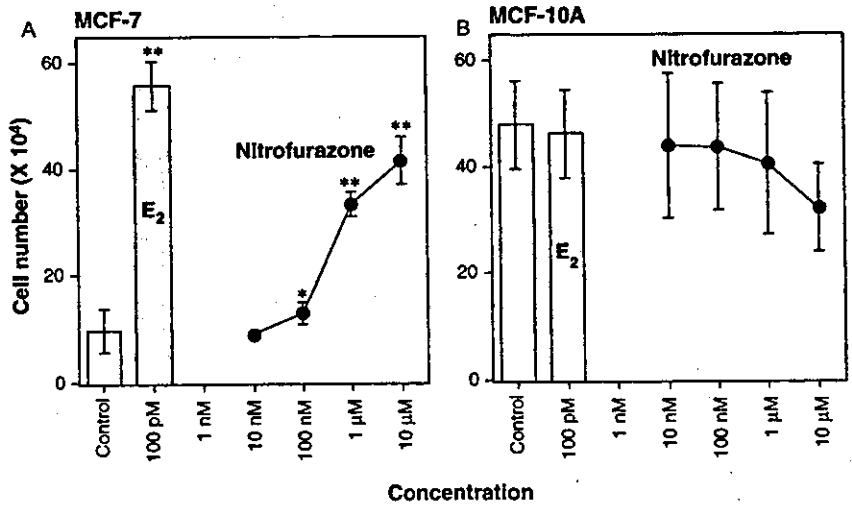

Fig. 1. Relative estrogenic activity of nitrofurazone. MCF-7 (A) or MCF-10A cells (B) were incubated with nitrofurazone for 6 days at 37 °C, and then harvested and counted. The data represent means ± SD of 6 (control and E_2) or 12 (nitrofurazone) independent experiments (A) or 8–9 experiments (B). *$P<0.05$ and **$P<0.001$, significantly increased compared with the control.

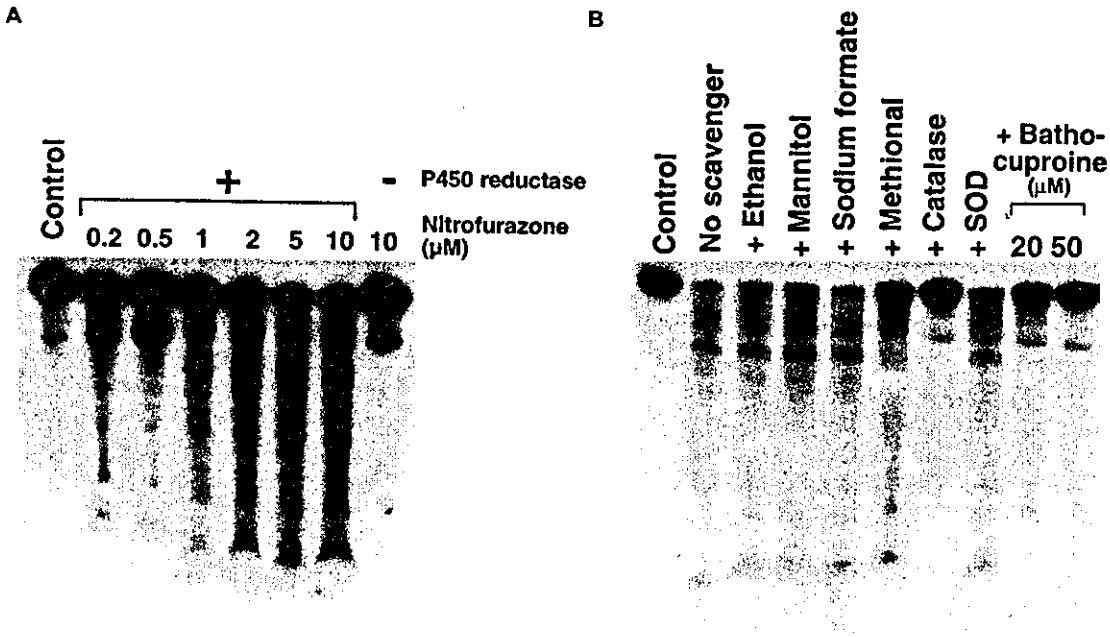

Fig. 2. Autoradiogram of ^{32}P-labeled DNA fragments incubated with nitrofurazone plus cytochrome P450 reductase, and effects of scavengers and bathocuproine. The standard reaction mixture, containing indicated concentration (A) or 1 μM (B) nitrofurazone, 100 μM NADPH and 2.1 μg/ml cytochrome P450 reductase in 20 mM potassium phosphate buffer (pH 7.4), was preincubated for 30 min at 25 °C. Then, ^{32}P-5′-end-labeled 211-base pair (A) or 443-base pair (B) DNA fragment, 10 μM/base sonicated calf thymus and 20 μM $CuCl_2$ were added, and the mixture was incubated for 60 min (A) or 30 min (B) at 37 °C. DNA fragments were electrophoresed on an 8% polyacrylamide/8 M urea gel. The autoradiogram was obtained by exposing an X-ray film to the gel. (B) Scavenger or bathocuproine was added after preincubation as follows, 5% (v/v) ethanol; 0.1 M mannitol; 0.1 M sodium formate; 0.1 M methional; 150 units/ml catalase; 150 units/ml SOD; 20 or 50 μM bathocuproine. Control contained none of nitrofurazone, $CuCl_2$ or cytochrome P450 reductase.

3.4. 8-oxodG formation in calf thymus DNA

Fig. 4 shows 8-oxodG formation induced by nitrofurazone treated with cytochrome P450 reductase. In the presence of both cytochrome P450 reductase and Cu(II), the amount of 8-oxodG increased depending on nitrofurazone concentrations. Nitrofurazone significantly increased 8-oxodG formation at 1 μM. In the absence of Cu(II), nitrofurazone did not increase the amount of 8-oxodG.

3.5. 8-oxodG formation in human cultured cells

Fig. 5 shows 8-oxodG formation in HL-60 cells treated with nitrofurazone. The amount of 8-oxodG in the cells significantly increased by 50 μM nitrofurazone compared with the control ($P<0.05$, Fig. 5). 8-oxodG formation returned to the control level at 100 μM (Fig. 5). This result suggests that optimal concentration of nitrofurazone causes oxidative damage to cellular DNA.

3.6. Generation of radicals by reduction of nitrofurazone

Fig. 6 shows ESR spectra of a radical generated from nitrofurazone treated with cytochrome P450 reductase and NADPH. This signal could be assigned to the nitro anion radical by performing the computer simulation using the reported hyperfine coupling constant [$a^{N}_{NO_2}=1.109$ mT, $a^{H}_{4}=0.593$ mT, $a^{H}_{3}=0.151$ mT, $a^{N}_{CH=N}=0.244$ mT, $a^{H}_{CH=N}=0.117$ mT] [26]. No signal was observed when cytochrome P450 reductase, NADPH or nitrofurazone was omitted (Fig. 6).

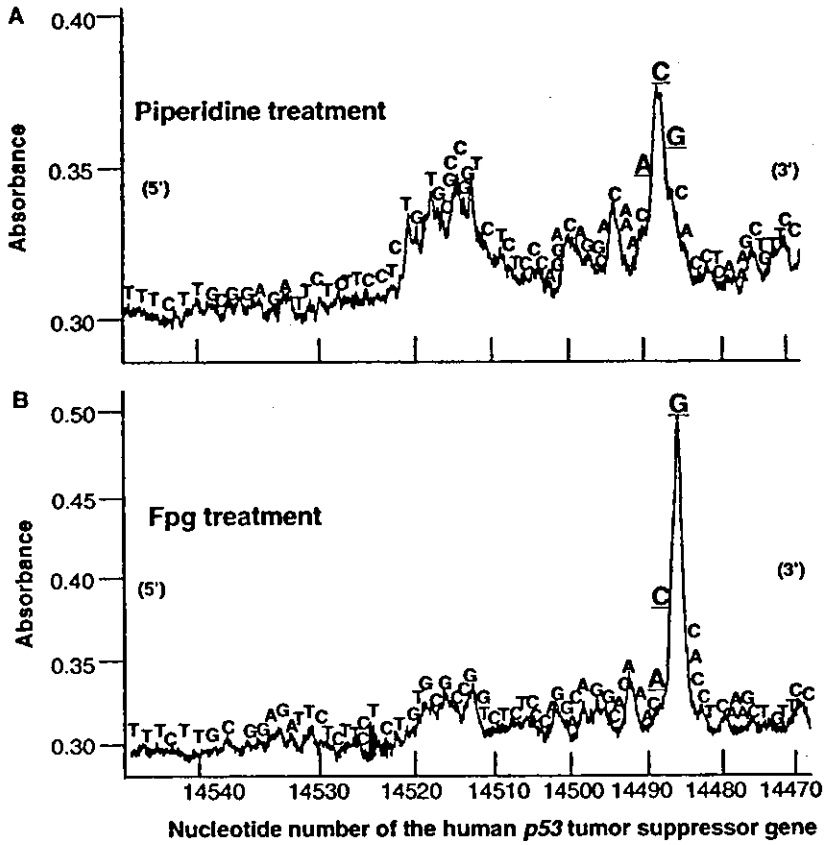

Fig. 3. Site specificity of piperidine-labile and Fpg-sensitive lesions formed by nitrofurazone. The standard reaction mixture containing 1 μM nitrofurazone, 100 μM NADPH and 2.1 μg/ml rat cytochrome P450 reductase in 20 mM potassium phosphate buffer (pH 7.4), was preincubated for 30 min at 25 °C. Then, ^{32}P-5′-end-labeled 443-base pair DNA fragment, 10 μM/base sonicated calf thymus and 20 μM $CuCl_2$ were added, and the mixture was incubated for 30 min at 37 °C. DNA fragments were treated with 1 M piperidine for 20 min at 90 °C (A), or 6 units of Fpg protein for 2 h at 37 °C (B). The relative amounts of DNA fragments were measured by scanning the autoradiogram with a laser densitometer. The horizontal axis shows the nucleotide number of the human *p53* tumor suppressor gene.

4. Discussion

The present study has shown that carcinogenic nitrofurazone is capable of inducing proliferation of estrogen-dependent cells. We firstly demonstrated that nitrofurazone significantly stimulated the proliferation of estrogen-dependent MCF-7 cells. Estrogens are highly mitogenic in hormone-sensitive tissues, such as uterus and breast [27]. Estrogens bind to estrogen receptors and thus initiate gene expression to regulate the cell cycle and cell proliferation [28]. Prolonged exposure of target tissues to excessive mitogenic stimulation by estrogens is considered to be important for the induction of cancer [27]. Estrogenic agents cause cancer particularly in female reproductive organs. Estrogenic soy isoflavones, genistein and daidzein, can cause cancer of reproductive organs such as uterus and vulva in rodents [29,30]. Recently, we have reported that cell proliferative activity of these isoflavones is attributed to binding of isoflavone-liganded estrogen receptors to estrogen response elements [17]. Nitrofurazone induces ovarian and mammary tumors in animals [1,7–10]. Thus, it is reasonably explained by assuming that nitrofurazone could act as a tumor promoter through its estrogenic action. This idea is confirmed by the finding that nitrofurazone as well as E_2 showed proliferative activity in estrogen receptor-positive

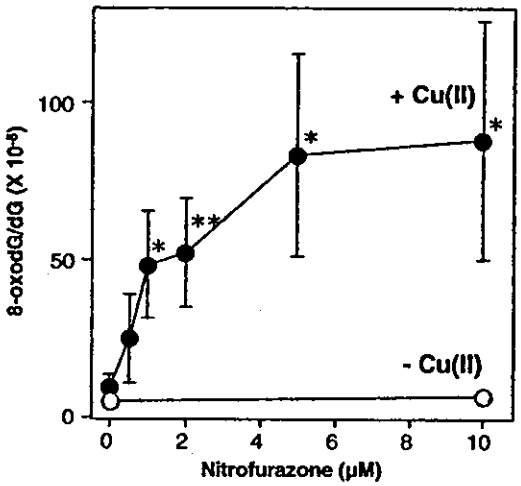

Fig. 4. Formation of 8-oxodG induced by nitrofurazone. The standard reaction mixture containing nitrofurazone, 100 μM NADPH and 2.1 μg/ml rat cytochrome P450 reductase in 4 mM potassium phosphate buffer (pH 7.4), was preincubated for 30 min at 25 °C. Then, 100 μM/base calf thymus DNA and no (open circle) or 20 μM $CuCl_2$ (closed circle) were added, and then the mixture was incubated for 30 min at 37 °C. After the incubation, 0.1 mM DTPA was added to stop the reaction. DNA was enzymatically digested into the nucleosides, and then, the amount of 8-oxodG was measured with an HPLC-ECD. The data represent means±SD of five independent experiments. $^{*}P<0.05$ and $^{**}P<0.01$, significantly increased compared with the control.

MCF-7 cells but not in estrogen receptor-negative MCF-10A cells.

In the present study, nitrofurazone caused damage to isolated and cellular DNA. Nitrofurazone caused Cu(II)-mediated oxidative damage to isolated DNA fragments only when cytochrome P450 reductase was added. A variety of nitro compounds are metabolized by cytochrome P450 reductase [11], and metabolites of certain nitro compounds can cause DNA damage [31,32]. Therefore, reductive activation of nitrofurazone appears to be required for DNA damage and subsequent mutation and carcinogenesis. Catalase and bathocuproine inhibited nitrofurazone-induced DNA damage, suggesting that H_2O_2 and Cu(I) are involved. Therefore, it is considered that H_2O_2 reacts with Cu(I) to produce the primary reactive species, such as the Cu(I)-hydroperoxo complex, capable of causing DNA damage. This hypothesis is supported by a previous study showing that superoxide anion radical (O_2^-), which is dismutated to H_2O_2, is produced during metabolic activation of nitrofurazone [33]. Although typical $^{\cdot}OH$ scavengers showed no inhibitory effect on DNA damage, the possibility that $^{\cdot}OH$ is generated from the DNA-Cu(I)-hydroperoxo complex and attacks DNA bases before scavengers react with $^{\cdot}OH$ cannot be excluded [34]. The proposed mechanism of DNA damage induced by nitrofurazone is shown in Fig. 7. Nitrofurazone undergoes cytochrome P450 reductase-catalyzed reduction to the corresponding nitro anion radical. One-electron reduction of nitrofurazone is confirmed by the finding that the ESR signal of this nitro anion radical was observed in the presence of both cytochrome P450 reductase and NADPH. This radical reacts with molecular O_2 to regenerate nitrofurazone with concomitant O_2^- production, resulting in the formation of a redox cycle. Formation of the redox cycle results in enhanced generation of reactive oxygen species and oxidative DNA damage, leading to carcinogenesis. In addition, the nitro compounds can be metabolized to corresponding hydroxylamine derivatives. Hydroxylamine derivatives are capable of causing oxidative DNA damage [31,35] and DNA adduct formation [36]. Thus, the possibility that DNA adduct formation by

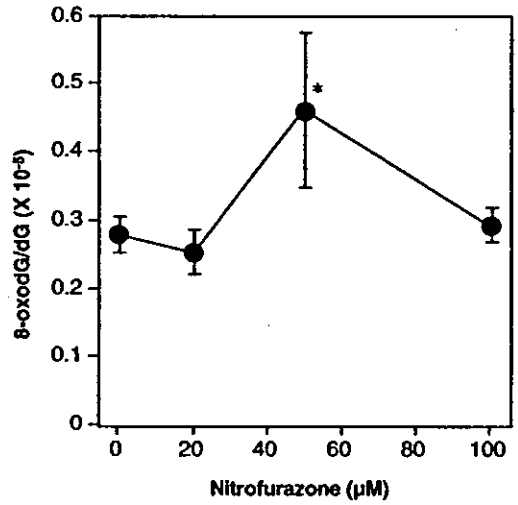

Fig. 5. Formation of 8-oxodG in cultured cells treated with nitrofurazone. HL-60 cells were incubated with various concentrations of nitrofurazone for 4 h at 37 °C. After the incubation, DNA was extracted and subjected to enzyme digestion, followed by analysis with an HPLC-ECD as described in Section 2. The data represent means±SD of 4 independent experiments. $^{*}P<0.05$, significantly increased compared with the control.

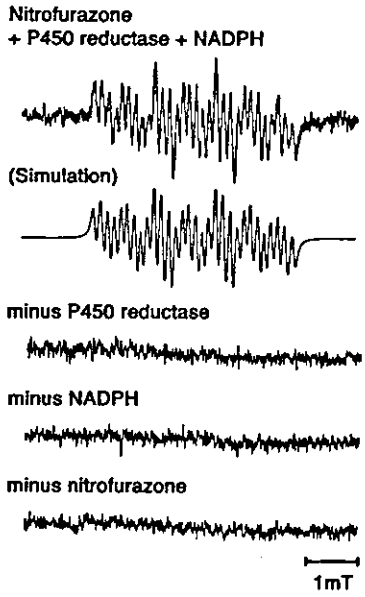

Fig. 6. ESR spectra and computer simulation of a radical derived from nitrofurazone treated with cytochrome P450 reductase. Reaction mixture containing 1 mM nitrofurazone, 1 mM NADPH and 4.2 μg/ml cytochrome P450 reductase in 100 mM potassium phosphate buffer (pH 7.4), was incubated for 5 min at 25 °C. Reaction mixtures were taken up capillary tubes and spectra were then measured.

hydroxylamine derivatives is involved in nitrofurazone-induced carcinogenesis cannot be excluded.

Piperidine and Fpg treatment detected nitrofurazone-induced cytosine and guanine damage to the 5′-A*CG*-3′ sequence complementary to codon 273, a well-known hotspot [37] of the *p53* tumor suppressor gene. Fpg protein catalyzes the excision of piperidine-resistant 8-oxodG [21], suggesting that 8-oxodG is formed at this hotspot. This finding is confirmed by the observation that 8-oxodG formation significantly increased in nitrofurazone-treated calf thymus DNA. The experiment using HL-60 cells shows that 8-oxodG formation should occur in cells exposed to nitrofurazone. The formation of 8-oxodG is known to cause G→T transversion, which might lead to mutation and subsequently cause cancer [38,39]. It is postulated that double-base lesions can be generated from one radical hit that leads through secondary reaction to a tandem base modification at pyrimidine and the adjacent guanine residues [40,41]. Furthermore, studies on site-specific DNA damage induced by nitrofurazone may provide an insight into estimation of reactive species, such as complexes of copper ions and H_2O_2 [42,43].

The necessity of Cu(II) in DNA damage has been identified by previous studies [44]. Copper occurs in the mammalian cell nucleus, and may contribute to high order chromatin structures [45]. Copper accumulation in the liver of Wilson's disease patients markedly increases the relative risk for primary liver cancer [46]. High concentrations of copper could induce cancer by damaging DNA [47,48]. It has been reported that copper has an ability to catalyze the generation of reactive oxygen species to cause DNA damage [49]. These studies support the finding that nitrofurazone metabolites caused DNA damage by generating reactive oxygen species through the interaction with copper.

In conclusion, nitrofurazone metabolites are involved in tumor initiation by causing oxidative DNA damage and nitrofurazone itself participates in tumor promotion and/or progression through enhancement of cell proliferation. In addition to nitrofurazone, various nitro compounds have been used as veterinary antimicrobial drugs [2–4]. Furazolidone and metronidazole induced mammary tumor in rats [2,4]. Nitrofurantoin induced ovarian tumor in mice and mammary tumors in rats [3]. Therefore, these nitro compounds may cause carcinogenesis in female reproductive organs in a similar manner to nitrofurazone.

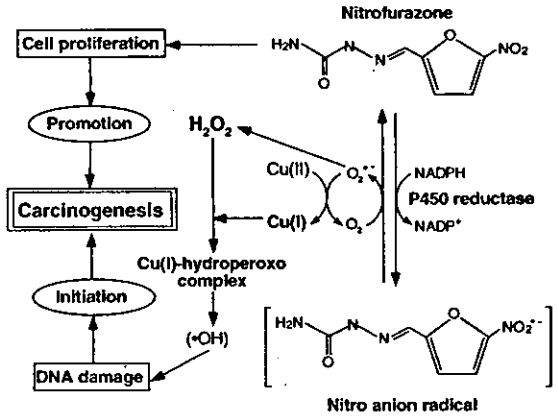

Fig. 7. Proposed mechanism of DNA damage and carcinogenesis induced by nitrofurazone.

Acknowledgements

This work was supported by Grants-in-Aid for Scientific Research from the Ministry of Education, Science, Sports and Culture of Japan.

References

[1] IARC Working Group, Nitrofural (nitrofurazone) in: IARC Monographs on the Evaluation of the Carcinogenic Risks of Chemicals to Humans, vol. 50, IARC, Lyon, 1990 pp. 195–209.
[2] IARC Working Group, Furazolidone in: IARC Monographs on the Evaluation of the Carcinogenic Risk of Chemicals to Humans, vol. 31, IARC, Lyon, 1983 pp. 141–151.
[3] IARC Working Group, Nitrofurantoin in: IARC Monographs on the Evaluation of the Carcinogenic Risks of Chemicals to Humans, vol. 50, IARC, Lyon, 1990 pp. 211–231.
[4] IARC Working Group, Metronidazole in: IARC Monographs on the Evaluation of the Carcinogenic Risks of Chemicals to Humans. Overall Evaluations of Carcinogenicity: an Updating of IARC Monographs 1 to 42, Suppl. 7, IARC, Lyon, 1987 p. 250.
[5] E.A. Sugden, A.I. Macintosh, A.B. Vilim, High pressure liquid chromatographic determination of nitrofurazone and furazolidone in chicken and pork tissues, J. Assoc. Off. Anal. Chem. 66 (1983) 874–880.
[6] A.B. Vilim, A.I. Macintosh, High pressure liquid chromatographic determination of nitrofurazone in milk, J. Assoc. Off. Anal. Chem. 62 (1979) 19–22.
[7] National Toxicology Program, Technical Report, Toxicology and carcinogenesis studies of nitrofurazone in F334/N rats and B6C3F1 mice, NTP TR-337, NIH Publication No. 88-2593, 1988.
[8] F.W. Kari, J.E. Huff, J. Leininger, J.K. Haseman, S.L. Eustis, Toxicity and carcinogenicity of nitrofurazone in F344/N rats and B6C3F1 mice, Food Chem. Toxicol. 27 (1989) 129–137.
[9] M. Takahashi, S. Iizuka, T. Watanabe, M. Yoshida, J. Ando, K. Wakabayashi, A. Maekawa, Possible mechanisms underlying mammary carcinogenesis in female Wistar rats by nitrofurazone, Cancer Lett. 156 (2000) 177–184.
[10] K. Takegawa, K. Mitsumori, K. Yasuhara, M. Moriyasu, M. Sakamori, H. Onodera, et al., A mechanistic study of ovarian carcinogenesis induced by nitrofurazone using rasH2 mice, Toxicol. Pathol. 28 (2000) 649–655.
[11] G. Sisson, A. Goodwin, A. Raudonikiene, N.J. Hughes, A.K. Mukhopadhyay, D.E. Berg, P.S. Hoffman, Enzymes associated with reductive activation and action of nitazoxanide, nitrofurans, and metronidazole in *Helicobacter pylori*, Antimicrob. Agents Chemother. 46 (2002) 2116–2123.
[12] B.A. Hoener, Nitrofurazone: kinetics and oxidative stress in the singlepass isolated perfused rat liver, Biochem. Pharmacol. 37 (1988) 1629–1636.
[13] P.L. Olive, Nitrofurazone-induced DNA damage to tissues of mice, Chem. Biol. Interact. 20 (1978) 323–331.
[14] IARC Working Group, IARC Monographs on the Evaluation of the Carcinogenic Risks of Chemicals to Humans in: Hormonal Contraception and Post-Menopausal Hormonal Therapy, vol. 72, IARC, Lyon, 1999.
[15] Y. Hiraku, N. Yamashita, M. Nishiguchi, S. Kawanishi, Catechol estrogens induce oxidative DNA damage and estradiol enhances cell proliferation, Int. J. Cancer 92 (2001) 333–337.
[16] A.M. Soto, C. Sonnenschein, K.L. Chung, M.F. Fernandez, N. Olea, F.O. Serrano, The E-SCREEN assay as a tool to identify estrogens: an update on estrogenic environmental pollutants, Environ. Health Perspect. 103 Suppl. 7 (1995) 113–122.
[17] M. Murata, K. Midorikawa, M. Koh, K. Umezawa, S. Kawanishi, Genistein and daidzein induce cell proliferation and their metabolites cause oxidative DNA damage in relation to isoflavone-induced cancer of estrogen-sensitive organs, Biochemistry 43 (2004) 2569–2577.
[18] Y. Kumagai, L.Y. Lin, A. Hiratsuka, S. Narimatsu, T. Suzuki, H. Yamada, et al., Participation of cytochrome P450-2B and 2D isozymes in the demethylenation of methylenedioxymethamphetamine enantiomers by rats, Mol. Pharmacol. 45 (1994) 359–365.
[19] P. Chumakov, EMBL Data Library, 1990, Accession number X54156.
[20] N. Yamashita, M. Murata, S. Inoue, Y. Hiraku, T. Yoshinaga, S. Kawanishi, Superoxide formation and DNA damage induced by a fragrant furanone in the presence of copper(II), Mutat. Res. 397 (1998) 191–201.
[21] M.H. David-Cordonnier, J. Laval, P. O'neill, Clustered DNA damage, influence on damage excision by XRS5 nuclear extracts and *Escherichia coli* Nth and Fpg proteins, J. Biol. Chem. 275 (2000) 11865–11873.
[22] A.M. Maxam, W. Gilbert, Sequencing end-labeled DNA with base-specific chemical cleavages, Methods Enzymol. 65 (1980) 499–560.
[23] H. Kasai, P.F. Crain, Y. Kuchino, S. Nishimura, A. Ootsuyama, H. Tanooka, Formation of 8-hydroxyguanine moiety in cellular DNA by agents producing oxygen radicals and evidence for its repair, Carcinogenesis 7 (1986) 1849–1851.
[24] K. Ito, S. Inoue, K. Yamamoto, S. Kawanishi, 8-Hydroxydeoxyguanosine formation at the 5′ site of 5′-GG-3′ sequences in double-stranded DNA by UV radiation with riboflavin, J. Biol. Chem. 268 (1993) 13221–13227.
[25] A. Furukawa, S. Oikawa, M. Murata, Y. Hiraku, S. Kawanishi, (−)-Epigallocatechin gallate causes oxidative damage to isolated and cellular DNA, Biochem. Pharmacol. 66 (2003) 1769–1778.
[26] D.N. Rao, R.P. Mason, Generation of nitro radical anions of some 5-nitrofurans, 2- and 5-nitroimidazoles by norepinephrine, dopamine, and serotonin. A possible mechanism for neurotoxicity caused by nitroheterocyclic drugs, J. Biol. Chem. 262 (1987) 11731–11736.
[27] B.T. Zhu, A.H. Conney, Functional role of estrogen metabolism in target cells: review and perspectives, Carcinogenesis 19 (1998) 1–27.

[28] J.G. Liehr, Is estradiol a genotoxic mutagenic carcinogen?, Endocr. Rev. 21 (2000) 40–54.
[29] J.E. Thigpen, J. Locklear, J.K. Haseman, H. Saunders, M.F. Grant, D.B. Forsythe, Effects of the dietary phytoestrogens daidzein and genistein on the incidence of vulvar carcinomas in 129/J mice, Cancer Detect. Prev. 25 (2001) 527–532.
[30] R.R. Newbold, E.P. Banks, B. Bullock, W.N. Jefferson, Uterine adenocarcinoma in mice treated neonatally with genistein, Cancer Res. 61 (2001) 4325–4328.
[31] S. Homma-Takeda, Y. Hiraku, Y. Ohkuma, S. Oikawa, M. Murata, K. Ogawa, et al., 2,4,6-Trinitrotoluene-induced reproductive toxicity via oxidative DNA damage by its metabolite, Free Radic. Res. 36 (2002) 555–566.
[32] M. Murata, Y. Yoshiki, M. Tada, S. Kawanishi, Oxidative DNA damage by a common metabolite of carcinogenic nitrofluorene and N-acetylaminofluorene, Int. J. Cancer 102 (2002) 311–317.
[33] J.F. Ghersi-Egea, V. Maupoil, D. Ray, L. Rochette, Electronic spin resonance detection of superoxide and hydroxyl radicals during the reductive metabolism of drugs by rat brain preparations and isolated cerebral microvessels, Free Radic. Biol. Med. 24 (1998) 1074–1081.
[34] M. Dizdaroglu, O.I. Aruoma, B. Halliwell, Modification of bases in DNA by copper ion-1,10-phenanthroline complexes, Biochemistry 29 (1990) 8447–8451.
[35] K. Sakano, S. Oikawa, Y. Hiraku, S. Kawanishi, Metabolism of carcinogenic urethane to nitric oxide is involved in oxidative DNA damage, Free Radic. Biol. Med. 33 (2002) 703–714.
[36] L. Fan, H.A. Schut, E.G. Snyderwine, Cytotoxicity, DNA adduct formation and DNA repair induced by 2-hydroxyamino-3-methylimidazo[4,5-*f*]quinoline and 2-hydroxyamino-1-methyl-6-phenylimidazo[4,5-*b*]pyridine in cultured human mammary epithelial cells, Carcinogenesis 16 (1995) 775–779.
[37] A.J. Levine, J. Momand, C.A. Finlay, The p53 tumour suppressor gene, Nature 351 (1991) 453–456.
[38] S.D. Bruner, D.P. Norman, G.L. Verdine, Structural basis for recognition and repair of the endogenous mutagen 8-oxoguanine in DNA, Nature 403 (2000) 859–866.
[39] S. Shibutani, M. Takeshita, A.P. Grollman, Insertion of specific bases during DNA synthesis past the oxidation-damaged base 8-oxodG, Nature 349 (1991) 431–434.
[40] A.G. Bourdat, T. Douki, S. Frelon, D. Gasparutto, J. Cadet, Tandem base lesions are generated by hydroxyl radical within isolated DNA in aerated aqueous solution, J. Am. Chem. Soc. 122 (2000) 4549–4556.
[41] H.C. Box, E.E. Budzinski, J.B. Dawidzik, J.S. Gobey, H.G. Freund, Free radical-induced tandem base damage in DNA oligomers, Free Radic. Biol. Med. 23 (1997) 1021–1030.
[42] K. Yamamoto, S. Kawanishi, Hydroxyl free radical is not the main active species in site-specific DNA damage induced by copper (II) ion and hydrogen peroxide, J. Biol. Chem. 264 (1989) 15435–15440.
[43] S. Frelon, T. Douki, A. Favier, J. Cadet, Hydroxyl radical is not the main reactive species involved in the degradation of DNA bases by copper in the presence of hydrogen peroxide, Chem. Res. Toxicol. 16 (2003) 191–197.
[44] A.M. Seacat, P. Kuppusamy, J.L. Zweier, J.D. Yager, ESR identification of free radicals formed from the oxidation of catechol estrogens by Cu^{2+}, Arch. Biochem. Biophys. 347 (1997) 45–52.
[45] M.J. Burkitt, Copper-DNA adducts, Methods Enzymol. 234 (1994) 66–79.
[46] H. Bartsch, J. Nair, Ultrasensitive and specific detection methods for exocylic DNA adducts: markers for lipid peroxidation and oxidative stress, Toxicology 153 (2000) 105–114.
[47] T. Theophanides, J. Anastassopoulou, Copper and carcinogenesis, Crit. Rev. Oncol. Hematol. 42 (2002) 57–64.
[48] H. Obata, N. Sawada, H. Isomura, M. Mori, Abnormal accumulation of copper in LEC rat liver induces expression of p53 and nuclear matrix-bound p21 (waf 1/cip 1), Carcinogenesis 17 (1996) 2157–2161.
[49] S. Kawanishi, Y. Hiraku, M. Murata, S. Oikawa, The role of metals in site-specific DNA damage with reference to carcinogenesis, Free Radic. Biol. Med. 32 (2002) 822–832.

Oxidative DNA Damage Induced by Benz[*a*]anthracene Dihydrodiols in the Presence of Dihydrodiol Dehydrogenase

Kazuharu Seike,[†,‡] Mariko Murata,[†] Kazutaka Hirakawa,[§,∥] Yoshihiro Deyashiki,[⊥] and Shosuke Kawanishi*[,†]

Department of Environmental and Molecular Medicine, Mie University School of Medicine, and Department of Radiation Chemistry, Life Science Research Center, Mie University, Tsu, Mie 514-8507, Japan, and Laboratory of Biochemistry, Gifu Pharmaceutical University, Gifu 502-8585, Japan

Received April 29, 2004

Tobacco smoke and polluted air are risk factors for lung cancer and contain many kinds of polycyclic aromatic hydrocarbons (PAHs) including benzo[*a*]pyrene (B[*a*]P) and benz[*a*]-anthracene (BA). BA, as well as B[*a*]P, is assessed as probably carcinogenic to humans (IARC group 2A). BA is metabolized to several dihydrodiols. Dihydrodiol dehydrogenase (DD), a member of the aldo-keto reductase superfamily, catalyzes $NAD(P)^+$-linked oxidation of dihydrodiols of aromatic hydrocarbons to corresponding catechols. To clarify the role of DD on PAH carcinogenesis, we examined oxidative DNA damage induced by *trans*-dihydrodiols of BA and B[*a*]P treated with DD using ^{32}P-5′-end-labeled DNA fragments obtained from the human *p53* tumor suppressor gene. In addition, we investigated the formation of 8-oxo-7,8-dihydro-2′-deoxyguanosine (8-oxodG), an indicator of oxidative DNA damage, in calf thymus DNA by using HPLC with an electrochemical detector. DD-catalyzed BA−1,2-dihydrodiol caused Cu(II)-mediated DNA damage including 8-oxodG formation in the presence of NAD^+. BA−1,2-dihydrodiol induced a Fpg sensitive and piperidine labile G lesion at the 5′-ACG-3′ sequence complementary to codon 273 of the human *p53* tumor suppressor gene, which is known as a hotspot. DNA damage was inhibited by catalase and bathocuproine, suggesting the involvement of H_2O_2 and Cu(I). The observation of NADH production by UV−visible spectroscopy suggested that DD catalyzed BA−1,2-dihydrodiol most efficiently to the corresponding catechol among the PAH−dihydrodiols tested. A time-of-flight mass spectroscopic study showed that the catechol form of BA−1,2-dihydrodiol formed after DD treatment. In conclusion, BA−1,2-dihydrodiol can induce DNA damage more efficiently than B[*a*]P−7,8-dihydrodiol and other BA−dihydrodiols in the presence of DD. The reaction mechanism on oxidative DNA damage may be explained by theoretical calculations with an enthalpy change of dihydrodiols and oxidation potential of their catechol forms. DD may play an important role in BA carcinogenesis via oxidative DNA damage.

Introduction

Exposure to tobacco smoke and pollutants has long been known as the major risk factor for the development of lung cancer (*1*). Tobacco smoke and polluted air contain many kinds of polycyclic aromatic hydrocarbons (PAHs) including benzo[*a*]pyrene (B[*a*]P) and benz[*a*]anthracene (BA). PAHs exert mutagenicity and carcinogenicity after metabolic activation (*2*−*4*). BA, as well as B[*a*]P, has been classified as a group 2A carcinogen, which is probably carcinogenic to humans, by the International Agency for Research on Cancer (IARC) (*2*, *5*). BA produced hepatomas and lung adenomas following repeated oral administration to mice (*5*). In addition, BA is a complete skin carcinogen (*5*). BA is metabolized to the 1,2-, 3,4-, 5,6-, 8,9-, and 10,11-dihydrodiols (*2*, *6*). Dihydrodiol dehydrogenase (DD; EC 1.3.1.20), a member of the aldo-keto reductase (AKR) superfamily, catalyzes $NAD(P)^+$-linked oxidation of *trans*-dihydrodiols of aromatic hydrocarbons to corresponding catechols. The enzyme is involved in the production of genotoxic *o*-quinone, which can induce DNA damage through autoxidation of its catechol intermediates (*7*). Relevantly, it is suggested that overexpression of DD is assosiated with lung cancer and hepatocellular carcinoma (*8*, *9*). These studies on DD let us consider the significance of oxidative DNA damage in PAH carcinogenesis, although DNA adduct formation is the most widely accepted mechanism.

To clarify the role of DD on PAH carcinogensis, we examined oxidative DNA damage and its site specificity induced by *trans*-dihydrodiols of BA and B[*a*]P treated with DD using ^{32}P-5′-end-labeled DNA fragments obtained from the human *p53* tumor suppressor gene. In addition, we investigated the formation of 8-oxo-7,8-dihydro-2′-deoxyguanosine (8-oxodG), an indicator of

* To whom correspondence should be addressed. Tel. and Fax: (+81) (59) 231 5011. E-mail: kawanisi@doc.medic.mie-u.ac.jp.
† Mie University School of Medicine.
‡ Present address: National Institute of Advanced Industrial Science and Technology, Research Center for Glycoscience, Cell Regulation Analysis Team, Tsukuba, Ibaraki 305-8562, Japan.
§ Mie University.
∥ Present address: Division of Applied Science and Basic Engineering, Faculty of Engineering, Shizuoka University, Hamamatsu, Shizuoka 432-8561, Japan.
⊥ Gifu Pharmaceutical University.

10.1021/tx0498814 CCC: $27.50
Published on Web 10/02/2004

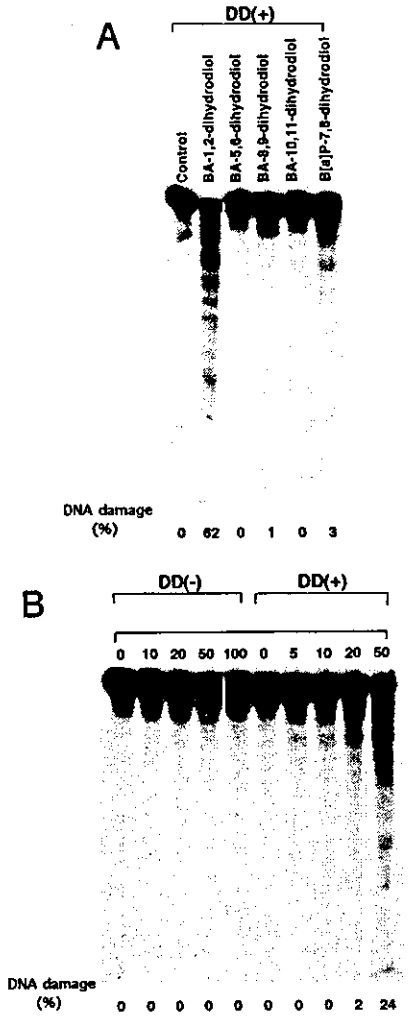

Figure 1. Autoradiogram of ^{32}P-labeled DNA fragments incubated with BA-dihydrodiols and B[*a*]P-7,8-dihydrodiol. (A) The reaction mixtures (in a 1.5 mL Eppendorf microtube) containing 100 μM BA-dihydrodiols and B[*a*]P-7,8-dihydrodiol with 9.6×10^{-3} U/mL DD and 100 μM NAD$^+$ were preincubated in 10 mM sodium phosphate buffer (pH 7.8) containing 5 μM DTPA at 37 °C for 1 h. (B) Another reaction mixture containing the indicated concentrations of BA-1,2-dihydrodiols with 9.6×10^{-3} U/mL DD and 100 μM NAD$^+$ was preincubated in 10 mM sodium phosphate buffer (pH 7.8) containing 5 μM DTPA at 37 °C for 30 min. After preincubation, ^{32}P-5′-end-labeled DNA fragments, calf thymus DNA (20 μM/base), and 20 μM $CuCl_2$ were added to the mixtures (200 μL), followed by the incubation at 37 °C for 1 h. After piperidine treatment, DNA was electrophoresed on an 8% polyacrylamide/8 M urea gel in Tris borate/EDTA buffer. The autoradiogram was obtained by exposing X-ray film to the gel. The percentage of DNA damage was roughly estimated by using a laser densitometer.

oxidative DNA damage, in calf thymus DNA by using an electrochemical detector coupled to HPLC (HPLC-ECD). We examined the conversion of NAD$^+$ to NADH during the reaction that DD catalyzes PAH–dihydrodiols to PAH–catechols by UV–visible spectroscopy. We detected the product in the enzymatic reaction of BA–1,2-dihydrodiol with DD in the presence of NAD$^+$, by using time-of-flight mass spectroscopy (TOF-MS). The reaction mechanism was discussed on the basis of theoretical calculations.

Materials and Methods

Materials. Restriction enzymes (*Apa*I, *Eco*RI, and *Hind*III) and alkaline phosphatase from calf intestine were purchased

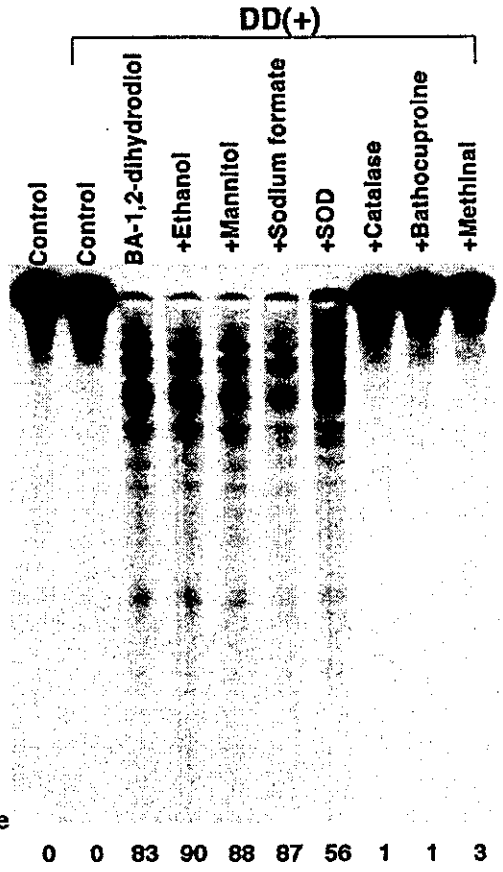

Figure 2. Effects of scavengers and a metal chelator on DNA damage induced by BA-1,2-dihydrodiol in the presence of Cu(II), DD, and NAD$^+$. The reaction mixtures containing the ^{32}P-5′-end-labeled 443 bp DNA fragments, calf thymus DNA (20 μM/base), 20 μM $CuCl_2$, 9.6×10^{-3} U/mL DD, 100 μM NAD$^+$, and 50 μM BA-1,2-dihydrodiol in 200 μL of 10 mM sodium phosphate buffer (pH 7.8) containing 5 μM DTPA were incubated at 37 °C for 1 h, after preincubation for enzymatic reaction (37 °C, 30 min). Ethanol (5%), mannitol (0.1 M), sodium formate (0.1 M), SOD (150 units/mL), catalase (150 units/mL), bathocuproine (50 μM), or methional (0.1 M) was added before the incubation. The DNA fragment was treated as described in the legend to Figure 1.

from Boehringer Mannheim GmbH (Mannheim, Germany). T_4 polynucleotide kinase was obtained from New England Biolabs (Beverly, MA). [γ-^{32}P]ATP (222 TBq/mmol) was acquired from Amersham Biosciences (Buckinghamshire, United Kingdom). Diethylenetriamine-*N*,*N*,*N*′,*N*″,*N*″-pentaacetic acid (DTPA) and bathocuproinedisulfonic acid were procured from Dojin Chemical Co. (Kumamoto, Japan). Acrylamide, piperidine, dimethyl sulfoxide (DMSO), bisacrylamide, and β-nicotinamide adenine dinucleotide (oxidized form) (NAD$^+$), were obtained from Wako Pure Chemical Industries, Ltd. (Osaka, Japan). $CuCl_2$, ethanol, D-mannitol, and sodium formate were acquired from Nacalai Tesque (Kyoto, Japan). BA–1,2-dihydrodiol, BA–3,4-dihydrodiol, BA–5,6-dihydrodiol, BA–8,9-dihydrodiol, BA–10,11-dihydrodiol, and B[*a*]P–7,8-dihydrodiol were obtained from Midwest Research Institute (Kansas City, MO). Calf thymus DNA, calf intestine phosphatase, superoxide dismutase (SOD, 3000 units/mg from bovine erythrocytes), and catalase (45000 units/mg from bovine liver) were obtained from Sigma Chemical Co. (St. Louis, MO). α-Cyano-4-hydroxycinnamic acid was procured from Sigma-Aldrich Japan K. K. (Tokyo, Japan). Nuclease P_1 (400 units/mg) was purchased from Yamasa Shoyu Co. (Chiba, Japan). *Escherichia coli* formamidopyrimidine-DNA glycosylase (Fpg) was obtained from Trevigen Inc. (Gaithersburg, MD).

Preparation of DD. DD, recombinant AKR1C22, belongs to a member of the AKR superfamily and was expressed in *E. coli* and purified to homogeneity as previously described (7). The

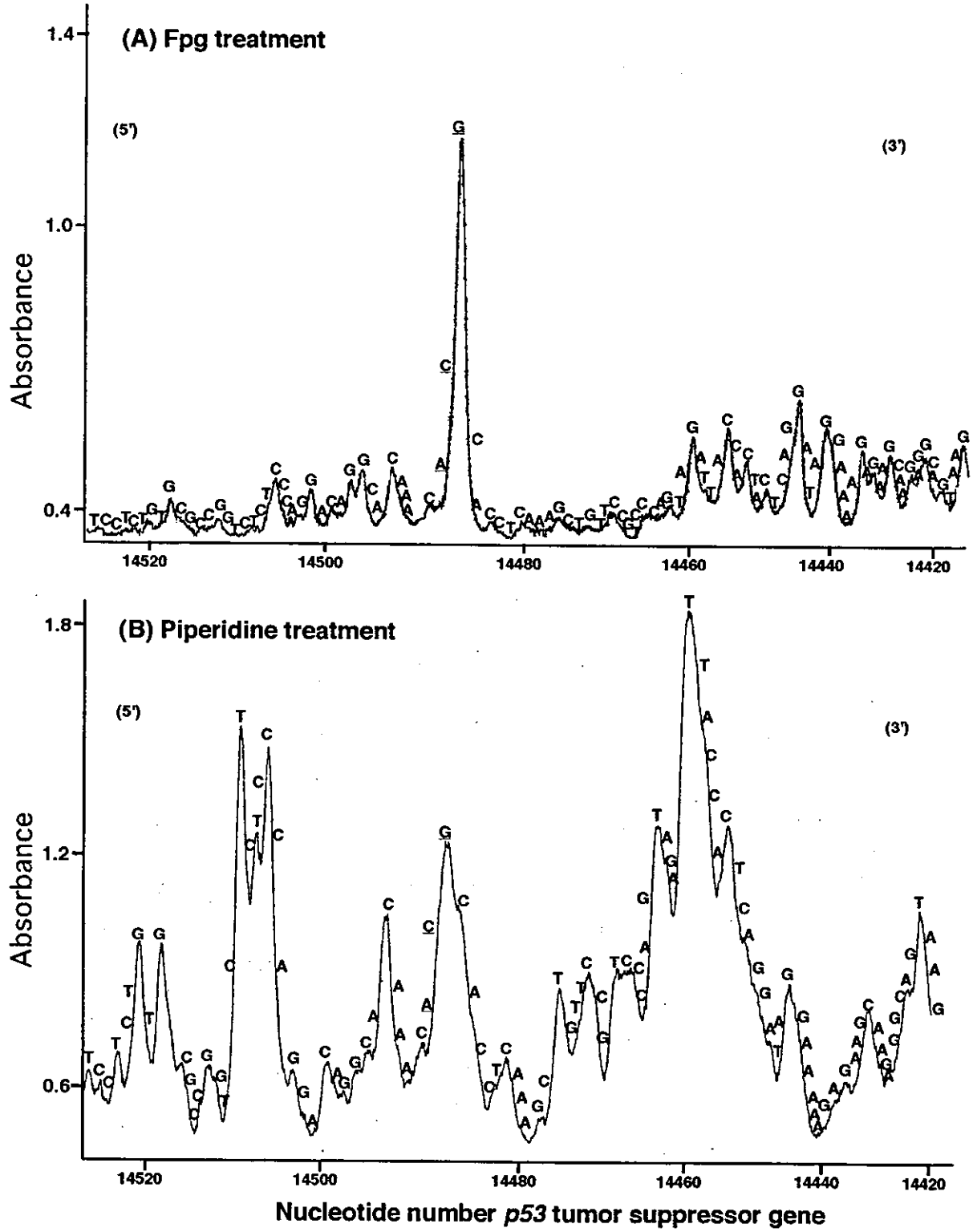

Figure 3. Site specificity of DNA damage induced by BA-1,2-dihydrodiol treated with DD. The reaction mixtures contained ^{32}P-5′-end-labeled 443bp (*Apa*I 14179-*Eco*R* I14621) DNA fragments of the *p*53 tumor suppressor gene, calf thymus DNA (20 μM/base), 20 μM $CuCl_2$, 9.6 × 10^{-3} U/mL DD, 100 μM NAD^+, and 50 μM BA-1,2-dihydrodiol in 200 μL of 10 mM sodium phosphate buffer (pH 7.8) containing 5 μM DTPA (preincubation, 37 °C, 30 min; incubation, 37 °C, 1 h). After Fpg (A) or piperidine (B) treatment, the DNA fragment was treated as described in the Materials and Methods.

buffer of the preparation was replaced to 10 mM sodium phosphate buffer, pH 7.8, and stored at −20 °C until used for the experiments.

Preparation of ^{32}P-5′-End-Labeled DNA Fragments. DNA fragments were obtained from the human *p53* tumor suppressor gene (*10*). The DNA fragment of the *p53* tumor suppressor gene was prepared from pUC18 plasmid. A singly ^{32}P-5′-end-labeled 443 bp fragment (*Apa*I 14179-*Eco*RI* 14621) and a 211 bp fragment (*Hin*dIII* 13972-*Apa*I 14182) were obtained according to the method described previously (*11*). The asterisk indicates ^{32}P-labeling.

Detection of DNA Damage Induced by BA Metabolites. Standard reaction mixtures (in a 1.5 mL Eppendorf microtube) containing the indicated concentrations of BA−dihydrodiols and B[*a*]P−7,8-dihydrodiol with 9.6 × 10^{-3} U/mL DD and 100 μM NAD^+ were preincubated in 10 mM sodium phosphate buffer

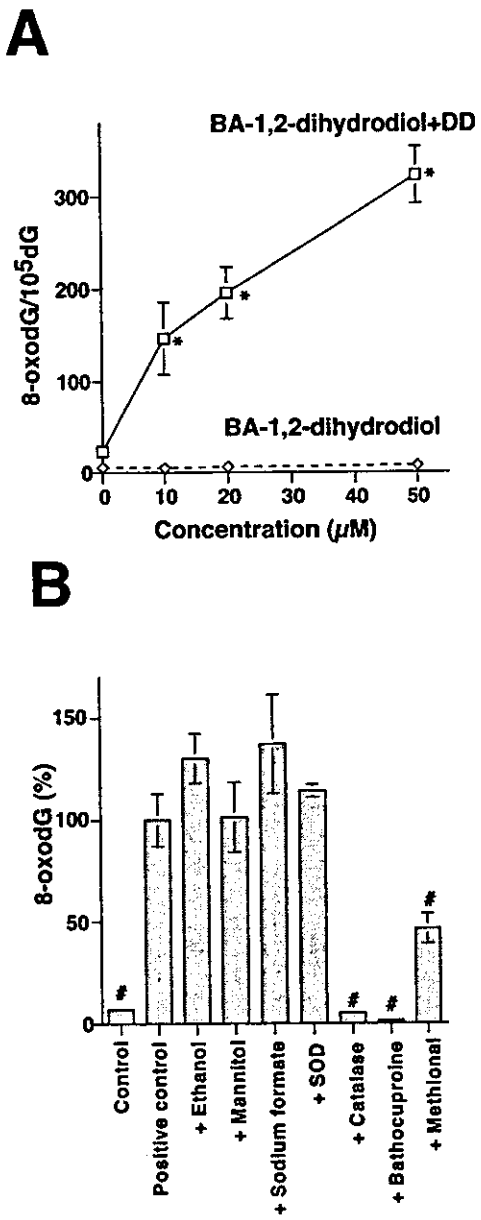

Figure 4. Formation of 8-oxodG in calf thymus DNA induced by BA-1,2-dihydrodiol treated with DD or not. (A) The reaction mixtures containing calf thymus DNA (100 μM/base), 20 μM $CuCl_2$, and 100 μM NAD^+ and the indicated concentrations of BA-1,2-dihydrodiol in 200 μL of 4 mM sodium phosphate buffer (pH 7.8) containing 5 μM DTPA with or without 9.6×10^{-3} U/mL DD were incubated at 37 °C for 1 h after preincubation for DD treatment (37 °C, 1 h). (B) The reaction mixtures containing calf thymus DNA (100 μM/base), 20 μM $CuCl_2$, 9.6×10^{-3} U/mL DD, 100 μM NAD^+, 50 μM BA-1,2-dihydrodiol, and the scavenger in 200 μL of 10 mM sodium phosphate buffer (pH 7.8) containing 5 μM DTPA were incubated at 37 °C for 1 h after preincubation for enzymatic reaction (37 °C, 1 h). Ethanol (5%), mannitol (0.1 M), sodium formate (0.1 M), SOD (150 units/mL), catalase (150 units/mL), bathocuproine (50 μM), or methional (0.1 M) was added before the incubation. The DNA fragment was enzymatically digested into the nucleoside, and 8-oxodG formation was analyzed by using the HPLC-ECD, as described in the Materials and Methods. The results are expressed as means and SD of values obtained from three independent experiments. Symbols indicate significant differences by Student's *t*-test (A, *; $P < 0.01$ as compared with control; B, #; $P < 0.01$ as compared with positive control).

(pH 7.8) containing 5 μM DTPA at 37 °C for 1 h. After preincubation,[32]P-5′-end-labeled DNA fragments, calf thymus DNA (20 μM/base), and 20 μM $CuCl_2$ were added to the mixtures (total 200 μL) followed by the incubation at 37 °C for 1 h. Then,

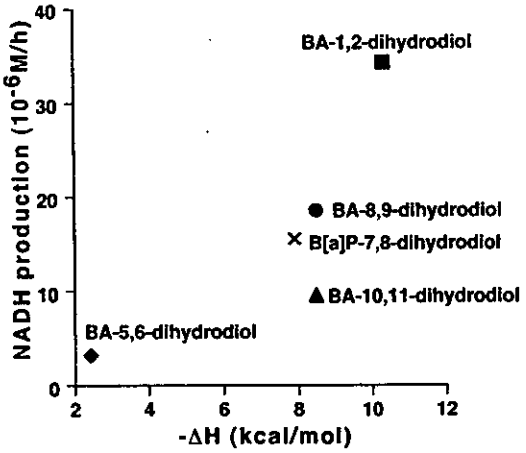

Figure 5. NADH formation in the reaction of NAD^+, BA-dihydrodiols, and DD. The reaction mixture containing 100 μM BA-dihydrodiols or B[*a*]P-dihydrodiol, 9.6×10^{-3} U/mL DD and 1 mM NAD^+, in 1000 μL of 10 mM sodium phosphate buffer (pH 7.8) was incubated at 37 °C for 1 h. The increase of absorbance at 340 nm for NADH during 1 h was calculated as the enzymatic activity.

the DNA fragments were treated in 10% (v/v) piperidine at 90 °C for 20 min or treated with 6 units of Fpg protein in 21 μL of reaction buffer [10 mM HEPES–KOH (pH 7.4), 100 mM KCl, 10 mM EDTA, and 0.1 mg/mL BSA] at 37 °C for 2 h. The treated DNA was electrophoresed on an 8% polyacrylamide/8 M urea gel. The autoradiogram was obtained by exposing X-ray film to the gel (*12*). The extent of DNA damage was roughly estimated by using a laser densitometer (LKB 2222 UltroScan XL). The preferred cleavage sites were determined by direct comparison of the positions of the oligonucleotides with those produced by the chemical reactions of the Maxam–Gilbert procedure (*13*) using a DNA sequencing system (LKB 2010 Macrophor). The laser densitometer was used for the measurement of the relative amounts of oligonucleotides from the treated DNA fragments.

Measurement of 8-OxodG Formation in Calf Thymus DNA. Reaction mixtures (in a 1.5 mL Eppendorf microtube) containing the indicated concentrations of BA–1,2-dihydrodiol were preincubated with 9.6×10^{-3} U/mL DD and 100 μM NAD^+ in 10 mM sodium phosphate buffer (pH 7.8) containing 5 μM DTPA at 37 °C for 30 min. Following the preincubation, DNA fragments (100 μM/base) from calf thymus and 20 μM $CuCl_2$ were added to the mixtures, incubated at 37 °C for 1 h. After ethanol precipitation, DNA was digested to nucleosides with nuclease P_1 and calf intestine phosphatase and analyzed by HPLC-ECD, as described previously (*14*).

UV–Visible Spectra Measurements. To examine the enzymatic activity, the UV–visible spectral change was measured with a UV–visible spectrometer (UV-2500PC; Shimadzu, Kyoto, Japan). The reaction mixture containing 100 μM BA–dihydrodiols, 1 mM NAD^+, and 9.6×10^{-3} U/mL DD in 1 mL of 10 mM sodium phosphate buffer (pH 7.8) containing 5 μM DTPA was incubated at 37 °C. The difference spectra between dihydrodiols/NAD^+/DD and dihydrodiols/NAD^+ were measured repeatedly at 37 °C for 1 h. The appearance of a new absorption at 340 nm ($\epsilon = 6.22 \times 10^3$ M^{-1} cm^{-1}) for NADH was assessed as the enzymatic activity. Theoretically, the corresponding catechols of dihydrodiols will yield at the equimolar amount of formed NADH.

TOF-MS Analysis. TOF-MS analysis was performed on a Voyager B-RP (PerSeptive Biosystems, Framingham, MA) equipped with a nitrogen laser (337 nm, 3 ns pulse) to determine the molecular weight of the product by the reaction of BA–1,2-dihydrodiol, DD, and NAD^+. Reaction mixtures containing 3 mM BA–1,2-dihydrodiol, 1.45×10^{-2} U/mL DD, and 3 mM NAD^+ in 132 μL of 3 mM sodium phosphate buffer (pH 7.8) were incubated at 37 °C for 1 h. Matrix solution (saturated α-cyano-4-hydroxycinnamic acid: 0.1%TFA/50%acetonitrile = 1:1) was

added to the sample and then air-dried on a stainless steel probe tip.

Calculation. The enthalpy change ($-\Delta H$) for dehydrogenation of BA−dihydrodiols and B[*a*]P−7,8-dihydrodiol was estimated from semiempirical calculation at PM3 level. Structures of these molecules were optimized by calculation of equilibrium geometry at the PM3 level. Energies of the highest occupied molecular orbital (HOMO) of dehydrogenated forms of BA−dihydrodiols and B[*a*]P−7,8-dihydrodiol were estimated from ab initio MO calculations at the Hartree−Fock 3-21G level. These calculations were performed utilizing Spartan '02 for Windows (Wavefunction Inc., CA).

Results

Damage to ^{32}P-Labeled DNA Fragments Induced by BA−Dihydrodiols. Figure 1A shows an autoradiogram of DNA damage by BA−dihydrodiols in the presence and absence of DD. Interestingly, BA−1,2-dihydrodiol induced Cu(II)-mediated DNA damage in the presence of DD but did not in the absence of DD. BA−1,2-dihydrodiol induced DNA damage more efficiently than B[*a*]P−7,8-dihydrodiol with metabolic activation. Other BA−dihydrodiols induced no DNA damage even in the presence of DD. BA−3,4-dihydrodiol induced Cu(II)-mediated DNA damage even in the absence of DD as reported previously (data not shown). Metabolically activated BA−1,2-dihydrodiol induced DNA damage in a dose-dependent manner (Figure 1B).

Effects of Scavengers and a Metal Chelator on DNA Damage Induced by BA−1,2-Dihydrodiol Treated with DD. Figure 2 shows the effects of scavengers and bathocuproine, a Cu(I) specific chelator, on DNA damage induced by BA−1,2-dihydrodiol treated with DD. Inhibition of DNA damage by catalase and bathocuproine suggests the involvement of hydrogen peroxide (H_2O_2) and Cu(I). Typical free hydoxyl radical (•OH) scavengers, such as ethanol, mannitol, and sodium formate, showed no inhibitory effects on DNA damage. Methional, which scavenges not only •OH but also crypto-OH radicals, inhibited DNA damage. SOD showed a partial inhibitory effect on DNA damage.

Site Specificity of DNA Damage by BA−1,2-Dihydrodiol in the Presence of DD. An autoradiogram was obtained and scanned with a laser densitometer to measure the relative intensity of DNA cleavage in the human *p53* tumor suppressor gene. With Fpg treatment, the DNA cleavage occurred mainly at guanine residues (Figure 3A). BA−1,2-dihydrodiol induced piperidine labile sites preferentially at thymine, cytosine, and guanine residues (Figure 3B). BA−1,2-dihydrodiol caused Fpg sensitive and piperidine labile lesions at G in the 5′-ACG-3′ sequence complementary to codon 273, a well-known hotspot of the *p53* tumor suppressor gene in lung cancer (*15*) (Figure 3A,B).

Formation of 8-OxodG by BA−1,2-Dihydrodiol in the Presence and Absence of DD. By using the HPLC-ECD, we measured the 8-oxodG content in calf thymus DNA treated with BA−1,2-dihydrodiol with or without DD (Figure 4A). BA−1,2-dihydrodiol significantly increased 8-oxodG formation in a dose-dependent manner in the presence of DD. In the absence of DD, BA−1,2-dihydrodiol did not increase the 8-oxodG formation. Figure 4B shows the inhibitory effects of scavengers on 8-oxodG formation induced by BA−1,2-dihydrodiol treated with DD. Catalase and bathocuproine completely inhibited 8-oxodG formation. Methional partially inhibited 8-oxodG formation.

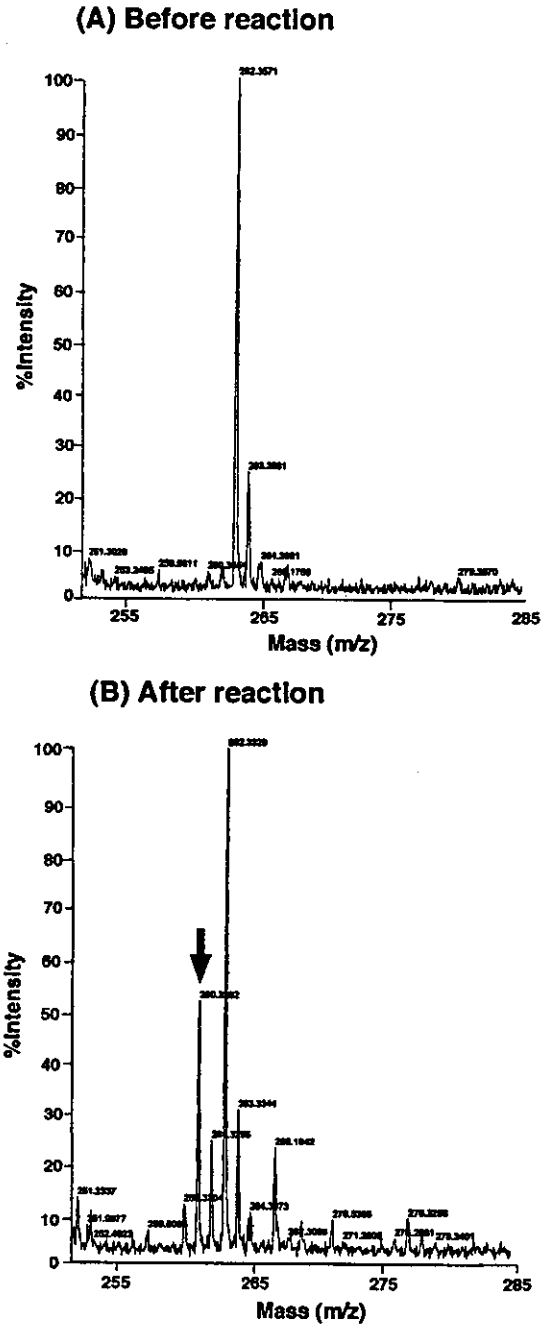

Figure 6. TOF-MS spectra of BA-1,2-dihydrodiol and its reaction product by DD. Reaction mixtures containing 3 mM BA-1,2-dihydrodiol, 1.45×10^{-2} U/mL DD, and 3 mM NAD^+ in 132 μL of 3 mM sodium phosphate buffer (pH 7.8) were incubated at 37 °C for 1 h. Matrix solution, saturated α-cyano-4-hydroxycinnamic acid:0.1%TFA/50%acetonitrile (1:1). Mass spectra show the products of BA-1,2-dihydrodiol before (A) and after reaction (B) with DD and NAD^+. The arrow indicates reaction product with *m/z* 260.

Enzymatic Activity of DD in the Aspect of Substrate Specificity. The DD activity of AKR1C22 for several dihydrodiols was spectrophotometrically measured as the increased absorbance of NADH at 340 nm. The formation rate of NADH was plotted against the calculated $-\Delta H$ for the dehydrogenation of dihydrodiols (Figure 5). The value of $-\Delta H$ implies the tendency to dehydrogenation of dihydrodiols to catechol. NADH production by DD appeared to increase depending on the